Available online at www.sciencedirect.com
ScienceDirect

Ceramics International 34 (2008) 1353–1360

CERAMICS INTERNATIONAL

www.elsevier.com/locate/ceramint

Theoretical analysis of colloidal interaction energy in nanoparticle suspensions

Kathy Lu [*]

Department of Materials Science and Engineering, Virginia Polytechnic Institute and State University, 213 Holden Hall-M/C 0237, Blacksburg, VA 24061, USA

Received 3 October 2006; received in revised form 8 December 2006; accepted 27 February 2007
Available online 10 May 2007

Abstract

This study is focused on understanding interaction energies for Al_2O_3 nanoparticle suspensions at high solids loadings. Among the four interaction energies: van der Waals interaction energy, electrostatic interaction energy, steric interaction energy, and depletion interaction energy, the study found that the van der Waals attraction is the dominant mechanism in destabilizing the dispersion system; the steric repulsion is a more effective stabilization mechanism than the electrostatic repulsion. The fundamental cause for an unstable suspension due to the particle–particle close contact and thus attraction at high solids loading can be overcome by increasing the particle–particle repulsion. When a dispersant is used in a suspension, the polymer chain length must be carefully selected so that the dispersant provides enough stabilization but does not compromise the maximum achievable solids loading. If an appropriate dispersant is chosen, up to 45 vol% solids loading suspension can be obtained for the Al_2O_3 nanoparticles.

Keywords: Nanoparticle; Suspension; Solids loading; Interaction energy

1. Introduction

Colloidal dispersion represents a state of higher free energy than aggregated state. Coagulation/flocculation, states of lower free energy, will occur spontaneously unless there is a substantial energy barrier preventing this tendency. In the presence of such a barrier, the system can remain stable for a long time. If conditions are adjusted so that the energy barrier is small enough, the colloid will become unstable. Generally, the dispersion will remain stable when the particle interaction energy barrier is several times of kT (k is Boltzmann constant and T is absolute temperature in Kelvin). When the interaction energy barrier is 1–2kT, the system will become unstable and coagulate/flocculate [1]. Thus, the whole question of colloidal stabilization is maintaining the interaction energy barriers between the particles.

For aqueous systems, the unique ionic properties of water allow addition of ions to overcome the problematic particle–particle attraction; this ion-related stabilizing mechanism is called electrostatic stabilization. Another approach is to add an ionic polymer dispersant to the suspension; polymer chains adsorb onto the particle surfaces and extend into water, and physically repel one another; this method of stabilization is called steric stabilization [2]. More effectively, an ionic polymer dispersant and the ionic properties of water can be used simultaneously to obtain a well-dispersed suspension; this method is called electrosteric stabilization [3]. A delicate balance must be maintained for the pH and the dispersant concentration of the suspension. Inappropriate pH will result in particle attraction, not repulsion [4]. The adsorbed polymer must be thick enough to prevent close particle contact and counteract the van der Waals forces. Too little polymer will cause bridging flocculation; too much polymer will cause depletion flocculation [5,6].

Ogden and Lewis [7] and Li and Lewis [8] studied adsorbed and non-adsorbed polymer effects on particle suspension and observed improved suspension stability at very low free polymer concentrations. Ideally, the adsorbed polymer layer should be just thick enough to prevent the van der Waals bonding. Since nanoparticles have much larger specific surface

---

[*] Tel.: +1 540 231 3225; fax: +1 540 231 8919.
E-mail address: klu@vt.edu.

0272-8842/$34.00 © 2007 Elsevier Ltd and Techna Group S.r.l. All rights reserved.
doi:10.1016/j.ceramint.2007.02.016

area than micron size particles, more polymer chains will be adsorbed to cover the nanoparticle surface of the same mass; this will correspondingly reduce the solids loading of the nanoparticle suspension. At the same time, nanoparticles have extremely large surface area and tend to aggregate instantaneously to reduce the surface energy, colloidal processing of nanoparticles by tailoring the particle surface properties is often the only viable approach. With the increasing reliance of dispersing nanoparticles in a suspension and converting the suspension into a monolithic shape, there is a need to examine colloidal nanoparticle interactions. The understanding in this area is particularly meaningful for high solid loading systems that will be formed into bulk shapes afterwards.

This paper is focused on understanding different interaction energies for Al_2O_3 nanoparticle suspensions at relatively high solids loadings through theoretical calculation and experimental result discussion. The relative importance of the interaction energies will be discussed. The relationships between colloidal processing conditions and the interaction energies will be established. The observation from this effort will be used to provide guidance for high solids loading nanoparticle suspension preparation with the ultimate goal of forming monolithic components.

2. Different types of interaction energy in Al_2O_3 nanoparticle suspensions

The theoretical analyses in this study are based on the colloidal systems prepared as follows. Al_2O_3 nanoparticles with specific surface area of 45 m^2/g (Nanophase Technologies, Romeoville, IL) were used for the dispersion study; the particle size distribution is 20–45 nm. Poly(acrylic acid) (PAA, M_w 1800, Aldrich, St. Louis, MO) and poly(methacrylic acid) (PMAA, M_w 15,000, Vanderbilt Co., Inc., Norwalk, CT) were used as polymer dispersants. HCl and NH_4OH solutions were used to adjust the suspension pH. To prepare Al_2O_3 suspensions, the Al_2O_3 nanoparticles were added for a specific solids loading in 10 g increments along with an appropriate amount of PMAA or PAA dispersant. Since low pH promotes dispersant adsorption onto Al_2O_3 nanoparticles, HCl solution was added to lower pH to 1.5 [9]. The suspension was ball milled for overnight with periodic adjustment of pH to 1.5. This procedure makes suspension of approximately 20 vol% Al_2O_3. NH_4OH was then used to adjust the suspension pH to 9.5. High pH induces full dissociation of the dispersants PMAA and PAA and creates mutual repulsion among the particles, resulting in better dispersion. Depending on the desired final solids loading, nano-Al_2O_3 was again added in 10 g increments, along with an appropriate amount of PMAA or PAA dispersant. The suspension was then mixed for 24 h for complete homogenization. The solids loading of the suspension was varied between 20 and 45 vol%. The isoelectric point is around pH 2–3 for both the PMAA and PAA suspensions as measured; repulsion exists among the nanoparticles for the studied pH range of 5.5–10.5 because of the negative zeta-potential of the nanoparticle surface. Potentiometric titration was used to determine the amount of the dispersant adsorbed onto the Al_2O_3 particles [10,11]; the adsorbed and free dispersants are a function of the suspension pH and the total amount of the dispersant. More experimental details can be found in prior publications [12,13].

Table 1
List of symbols used

Symbol	Representation
a_1, a_2, a	Particle radii
A	Hamaker constant
c	Molar concentration of ions
C	Constant
e	Electron charge
$E_T(h)$	Total interaction energy between nanoparticles
$E_{vdw}(h)$	van der Waals interaction energy between nanoparticles
$E_{es}(h)$	Electrostatic interaction energy between nanoparticles
$E_{ster}(h)$	Steric interaction energy between nanoparticles
$E_{dep}(h)$	Depletion interaction energy between nanoparticles
$E_{elastic}(h)$	Polymer chain elastic interaction energy
$E_{mix}(h)$	Mixing interaction energy
h	Particle–particle separation distance
k	Boltzmann constant
L	Adsorbed polymer layer thickness
M_w	Molecular weight of adsorbed polymer dispersant
M_s	Molecular weight of polymer repeating unit
N_A	Avogadro's number
p	Degree of interpenetration between free and adsorbed polymer chains
q	Compression of grafted polymer layer
R	Particle center-to-center distance
r	Number of statistical segments per polymer chain
s	Projected length of each repeating unit
T	Absolute temperature
V_f	Average volume fraction of polymer segments in adsorbed layer
z	Valence of ion
$1/\kappa$	Electrical double layer thickness
ε_r	Dielectric constant of suspension medium
ζ	Zeta-potential of suspension
ε_0	Permittivity of free space
ν	Molecular volume of dispersing medium
χ	Flory-Huggins parameter
ρ	Density of adsorbed polymer dispersant
ϕ_{eff}	Effective solids loading
ϕ	Particle solids loading
Δ	Depletion layer thickness
μ_1	Chemical potential at a volume fraction of free polymer ϕ_p
μ_1^0	Chemical potential of dispersing medium at $\phi_p = 0.0$

As well known, the van der Waals interaction is ubiquitous and this is no exception for the studied system. Since both dispersant and ions were used for the Al_2O_3 nanoparticle colloidal stabilization, the electrostatic and steric interactions can be expected. Also, free polymer was present in the suspensions at all pH levels. Based on these considerations, there are four possible interaction energies: van del Waals interaction energy ($E_{vdw}(h)$), electrostatic interaction energy ($E_{es}(h)$), steric interaction energy ($E_{ster}(h)$), and depletion interaction energy ($E_{dep}(h)$). A list of symbols used in this paper is given in Table 1. Even though it has been noted that the steric layer and the electric double layer are not independent [14], it is assumed here that different interaction energies are additive in order to estimate the stability of the suspension system. Ideally the total interaction energy $E_T(h)$ between the Al_2O_3 nanoparticles is the sum of the van der Waals ($E_{vdw}(h)$), electrostatic ($E_{es}(h)$), steric ($E_{ster}(h)$), and depletion ($E_{dep}(h)$) energies:

$$E_T(h) = E_{vdw}(h) + E_{es}(h) + E_{ster}(h) + E_{dep}(h) \tag{1}$$

h is the separation distance between Al_2O_3 nanoparticles, $E_{vdw}(h)$ and $E_{dep}(h)$ are attractive energies while $E_{es}(h)$ and $E_{ster}(h)$ are repulsive energies. The stability of the colloidal suspensions depends on the interaction of these different energies and the resultant magnitude of the total interaction energy $E_T(h)$.

2.1. van der Waals interaction

For the van der Waals interaction between two particles, theoretical derivation starts with the assumption that the particle separation distance h is much larger compared to the two particle radii a_1 and a_2 [15]. For spherical particles, the van der Waals interaction energy can be expressed as:

$$E_{vdw}(h) = -\frac{A}{6}\left\{\frac{2a_1a_2}{R^2-(a_1+a_2)^2} + \frac{2a_1a_2}{R^2-(a_1-a_2)^2} + \ln\left(\frac{R^2-(a_1+a_2)^2}{R^2-(a_1-a_2)^2}\right)\right\} \tag{2}$$

A is Hamaker constant, R is particle center-to-center distance. With the recognition that the two particles do not interact significantly until the distance of the closest approach h is small compared to the particle size, Hamaker considered the interaction energy per unit area of close particle–particle approach and derived the van der Waals interaction energy as [15]:

$$E_{vdw}(h) = -\frac{A}{12h}\left(\frac{2a_1a_2}{a_1+a_2}\right) \tag{3}$$

For the particles with the same radius a, Eq. (3) can be further simplified as:

$$E_{vdw}(h) = -\frac{Aa}{12h} \tag{4}$$

With the Hamaker approximation, Eqs. (3) and (4) have been applied to many particle suspension systems within nanometer range separation distance. However, particle–particle interaction is more accurately the interaction of the molecules comprised of the particles. Since molecular interactions occur by electromagnetic wave propagation, there is a delay between the wave being sent out by one molecule, its arrival at a neighboring molecule, and the response of that molecule being received by the first. Because the interaction between the colloidal particles has a much larger range than those between individual molecules, this delay has to be considered and is known as retardation effect. Gregory considered two particle interaction with retardation effect and expressed $E_{vdw}(h)$ in an improved format [16]:

$$E_{vdw}(h) = \frac{-Aa}{12h}\left[1 - \frac{5.32h}{100}\ln\left(1+\frac{100}{5.32h}\right)\right] \tag{5}$$

The underlying assumption for this expression is that the particle–particle interaction length scale is much smaller than the particle size and only stands when $h \ll a$. At larger particle–particle separation distance, the van der Waals interaction energy approaches zero. For the studied Al_2O_3 nanoparticle system, the particle–particle separation distance h is about 25% of the particle radius a if the particles are equally separated at 45 vol% solids loading. Theoretically, high solids loading such as 45 vol% is achievable. However, h can become much smaller than the particle radius a when the particles are not ideally separated due to thermal perturbation or particle collision. A cascade of such close approach events can cause coagulation/flocculation. To estimate the particle–particle interaction under the van der Waals effect, the Hamaker constant A can be obtained based on the Lifshitz theory when the dispersing medium is water, with the value of 3.67×10^{-20} J [17]. Based on these considerations, the van der Waals interaction energy change as a function of the particle–particle separation distance h can be calculated and the result is shown in Fig. 1. Since the van der Waals interaction is attractive, $E_{vdw}(h)$ is negative with infinite value as $h \to 0$ and diminishes quickly as h increases. Clearly, the whole process of the colloidal stabilization is to find ways to prevent the particle–particle attraction, especially when certain particles happen to approach each other too closely. If individual particles can be well separated and the energy barrier is established to counteract the attraction, there is ample opportunity for the creation of stable and high solids loading nanoparticle suspensions.

2.2. Electrostatic interaction

To provide a repulsion mechanism for the dispersed Al_2O_3 nanoparticles in preventing coagulation/flocculation, the first approach is to use electrolyte(s) to create an electric double layer on each particle surface. The formation and structure of the electric double layer have been well discussed in the literature. The core idea is that each particle surface carries the same electric charge and repels each other when the particles

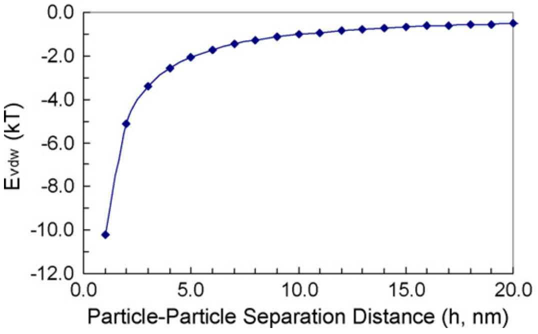

Fig. 1. The van der Waals interaction energy change vs. particle–particle separation distance h in the studied Al_2O_3 nanoparticle systems.

approach closely. A good estimation of the electric double layer can be done using electric double layer thickness $1/\kappa$, which can be expressed as [18]:

$$\kappa = \left(\frac{2e^2 N_A (1/2 \sum c_i {z_i}^2)}{\varepsilon_0 \varepsilon_r kT} \right)^{\frac{1}{2}} \tag{6}$$

e is electron charge, N_A is Avogadro's number, c is the molar concentration of ions, z is the valence of each ion, ε_0 is the permittivity of free space ($8.854 \times 10^{-12}\,\mathrm{F\,m^{-1}}$), ε_r is the dielectric constant of the suspension medium and is approximately 78.40 for an aqueous system at 20 °C [19]. Since HCl and NH_4OH were used to adjust the suspension pH for the studied Al_2O_3 nanoparticle system, z is 1 and c can be determined by the amount of HCl and NH_4OH used for each suspension. Eq. (6) can be further simplified at room temperature as [20]:

$$\kappa^{-1} = 0.1515 (C_{\mathrm{Cl}^-} + C_{\mathrm{NH}_4^+})^{-\frac{1}{2}} \tag{7}$$

C_{Cl^-} and $C_{\mathrm{NH}_4^+}$ are in mol/dm^3 and $1/\kappa$ is in nm. For the studied systems, κ has been calculated to be 1.82–2.98 nm^{-1} for the studied pH 5.5–10.5 range. Accordingly, $1/\kappa$ is about 0.3–0.6 nm from pH 5.5–10.5. Compared to the 27.5 nm Al_2O_3 particle size (13.75 nm for the particle radius a), the electric double layer will not substantially increase the effective solids loading (the sum of the Al_2O_3 nanoparticle solids loading and the electric double layer volume) in the suspension. Using the same Hamaker approximation approach for the van der Waals interaction energy, the repulsive potential energy can be calculated [15]. One requirement for this energy calculation is that the absolute particle surface potential should be <50 mV, for which the studied system is satisfactory with zeta-potential ζ at −43 mV or lower [12]. When $\kappa a > 10$, the electrostatic repulsion energy is [2,17]:

$$E_{es}(h) = 2\pi\varepsilon_r\varepsilon_0 a\zeta^2 \ln[1 + \exp(-\kappa h)] \tag{8}$$

When the electric double layer around the particles is very extensive such that $\kappa a < 5$, the procedure begins to break down. An approximate electrostatic repulsion energy expression can be obtained:

$$E_{es}(h) = 2\pi\varepsilon_r\varepsilon_0 a\zeta^2 [\exp(-\kappa h)] \tag{9}$$

Since κ ranges from 1.82 to 2.98 nm^{-1} and the Al_2O_3 particle radius a is ∼13.75 nm, κa is >10 and only Eq. (8) is applicable when calculating the electrostatic interaction energy. The zeta-potentials for different PAA and PMAA suspension systems are used accordingly and the values center around −40 mV. The result of the electrostatic interaction energy change versus the particle–particle separation distance h is shown in Fig. 2. Similar to the van der Waals interaction, the electrostatic interaction energy is mostly effective when the particle–particle separation distance is small. As the particle–particle separation distance h increases, the electrostatic repulsion $E_{es}(h)$ quickly approaches zero. For different κ, the electrostatic interaction energy varies. As the electric double layer thickness $1/\kappa$ increases, the repulsion between the particles increases and stays to be effective at larger particle–particle separation distance h. However, the electrostatic repulsion becomes negligible when h is greater than 3 nm under all studied conditions.

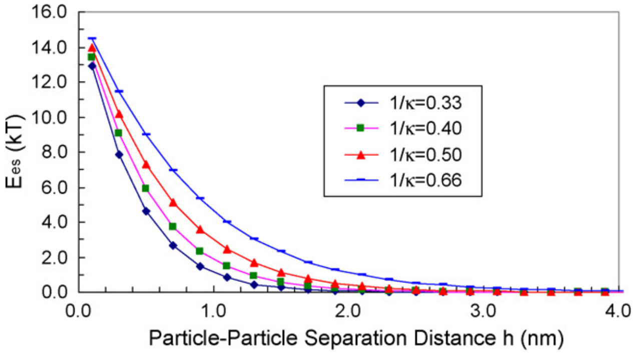

Fig. 2. The electrostatic interaction energy change vs. particle–particle separation distance h in the studied Al_2O_3 nanoparticle systems, $1/\kappa$ is in nm.

The effect of the electric double layer on the suspension solids loading can also be estimated. The thickest double layer $1/\kappa$ is calculated as 0.66 nm at pH 10.5, which will increase the particle size from 27.5 nm to 28.16 nm. As a result, the effective solids loading will increase to ∼48 vol% for the initially 45 vol% solids loading suspension. This new solids loading level is still far below the solids loading level achieved for micron size particles, usually ∼64 vol%. According to this estimate, the double layer for the electrostatic stabilization will not play any significant role in hindering the increase of the Al_2O_3 nanoparticle solids loading. Attentions should be focused on effectively utilizing the electrostatic stabilization mechanism to counteract the van der Waals attraction.

Under the general principle of achieving a stable yet simple suspension, it is much desired if the electrostatic stabilization mechanism alone can stabilize the Al_2O_3 nanoparticle system. The feasibility of doing so can be examined by summing the van der Waals and electrostatic interaction energies in Fig. 1 and 2 and the results are shown in Fig. 3. As it shows, the interaction energy is attractive at all particle–particle separation distances even though the magnitude is slightly smaller than

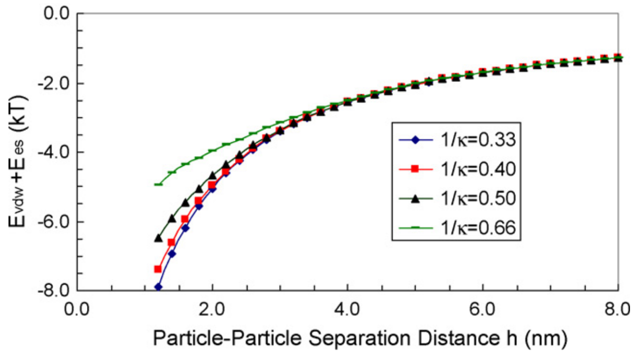

Fig. 3. The sum of the van der Waals and electrostatic interaction energy change vs. particle–particle separation distance h in the studied Al_2O_3 nanoparticle systems, $1/\kappa$ is in nm.

that without the electrostatic interaction; the overall attractive energy decreases as the electric double layer thickness $1/\kappa$ increases. This explains theoretically why it is impossible to create a stable Al_2O_3 nanoparticle suspension at the 20–45 vol% solids loading range. To create a stable Al_2O_3 nanoparticle suspension, the attractive energy has to be overcome. One possible solution is to increase the effect of the electrostatic stabilization mechanism by decreasing the electrolyte valance (z) and the concentration c. However, z is at the smallest value 1 with the use of HCl and NH_4OH and cannot be reduced any further. The only option is to lower the amount of HCl or NH_4OH used so that $1/\kappa$ can be further increased based on Eq. (7). However, the total electrolyte concentration has to be reduced to only ~1.6% of the current concentration in order to increase $1/\kappa$ to 3.0–5.0 nm range. This can create two problems: one is the ability of adjusting the suspension pH away from the pure Al_2O_3 isoelectric point (pH 8–9) and the other is maintaining high enough particle surface zeta-potential ζ (Eq. (8)). Otherwise, $E_{es}(h)$ will not be increased. Due to these constraints, tailoring the magnitude of the electrostatic stabilization energy is not an effective way to overcome the van der Waals interaction energy. Additional stabilization mechanism has to be introduced to promote a stable suspension. More effectively, a polymer dispersant can be introduced to adsorb onto the Al_2O_3 nanoparticle surfaces to provide a hindrance layer for attraction and also possibly electrostatic repulsion.

2.3. *Steric interaction energy*

The way polymer adsorbs onto particle surfaces depends on the chemical nature of the polymer chain, the nature of the particle surface, and the dispersing medium. Polymers typically adsorb at random points along their backbones; rarely do they collapse onto the particle surface by sacrificing entropy in the transition from three to two dimensions. Instead, the adsorbed chain consists of a collection of trains, loops, and tails. Besides the van der Waals and electrostatic interactions between the particles, the steric stabilization is often present when polymers are used to disperse the particles. Both mixing and steric repulsion energies are involved for the polymers attached to the particle surfaces in an aqueous suspension. If the adsorbed polymer layer thickness is L, there is no steric interaction between the two particles when h is $>2L$. For the interactions between the adsorbed polymer layers in the region $L < h < 2L$, where chain conformations from only trains and loops are taken into consideration, the mixing interaction energy $E_{mix}(h)$ is given by [21,22]:

$$E_{mix}(h) = \frac{32\pi kTa}{5\nu}\frac{V_f^2}{L^4}\left(\frac{1}{2}-\chi\right)\left(L-\frac{h}{2}\right)^6 \qquad (10)$$

where V_f is the average volume fraction of the polymer segments in the adsorbed layer, ν is the molecular volume of the dispersing medium, and χ is the Flory-Huggins parameter. At small particle–particle separation ($h < L$), the polymer segment density is assumed to be uniform and the contributions from the elastic and mixing interactions are given by:

$$E_{mix}(h) = \frac{4\pi akTL^2}{\nu}V_f^2\left(\frac{1}{2}-\chi\right)\left(\frac{h}{2L}-\frac{1}{4}-\ln\frac{h}{L}\right) \qquad (11)$$

$$E_{elastic}(h) = \frac{2\pi akTL^2\rho}{M_w}V_f^2\left\{\frac{h}{L}\ln\left[\frac{h}{L}\left(\frac{3-h/L}{2}\right)^2\right] - 6\ln\left(\frac{3-h/L}{2}\right)+3\left(1-\frac{h}{L}\right)\right\} \qquad (12)$$

$E_{elastic}(h)$ is the polymer chain elastic interaction energy, ρ is the density and M_w is the molecular weight of the adsorbed polymer dispersant. For the studied system, M_w is 1800 for PAA and 15,000 for PMAA. For the Al_2O_3 nanoparticle system, the steric interaction energy can be calculated based on $E_{mix}(h)$ and $E_{elastic}(h)$ at different particle–particle separation distance h. V_f and χ are assumed as 0.15 and 0.485 [22]. The only factor that substantially affects the steric interaction energy is the adsorbed polymer layer thickness L. L can be estimated based on the molecular weight M_w and the dynamic light scattering measurements as reported in the literature [3,5,10,23]:

$$L(\text{nm}) = 0.06(M_w)^{0.5} \qquad (13)$$

This estimation is well suited for PMAA and PAA as shown in the above references. Thus, the polymer adsorption layer thickness L in this study is estimated based on Eq. (13). L varies from 1.0 to 5.0 nm when M_w is changed from 270 to 7000. High M_w (such as 15,000) polymer effect can be easily calculated but the calculation here based on lower M_w will provide clear indication for the impact of higher M_w chain. The steric interaction energies for the Al_2O_3 nanoparticle system are shown in Fig. 4. Clearly, the adsorbed polymer layer thickness plays a substantial role in creating the steric repulsion between the particles. When the polymer layer thickness increases from 1.0 to 5.0 nm, the steric repulsion energy increases by almost 30 times. Also, the steric repulsion energy effective range increases drastically as the adsorbed polymer layer thickness increases. At 1.0 nm polymer adsorption thickness, the steric repulsion approaches zero at ~2.0 nm particle–particle separation distance. As the polymer adsorption thickness increases to 5.0 nm, the steric repulsion is effective up to ~6.0 nm.

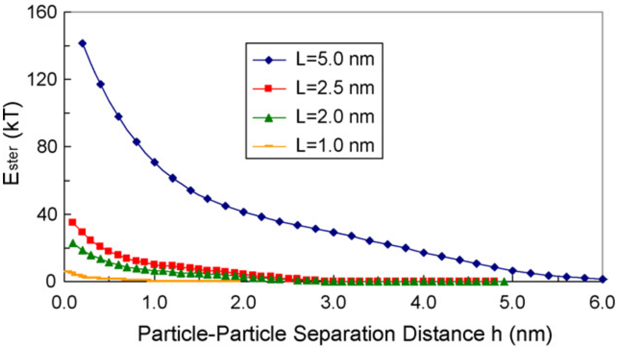

Fig. 4. The steric interaction energy change vs. particle–particle separation distance h in the studied Al_2O_3 nanoparticle systems.

While the adsorbed polymer is always beneficial for increasing the steric repulsion between the particles, the benefit can be compromised when the polymer chain is too short as shown in Fig. 4. The repulsion energy is low when the polymer adsorption layer thickness is 1.0 nm. An accompanying issue is that not all polymer chains will adsorb onto the particle surfaces. Some polymer chains will stay in the suspension as free polymer and cause depletion attraction between the particles. The shorter the polymer chain, the more likely there will be fewer adsorption points on the polymer backbone and thus more free polymers. Equally importantly, the impact of the adsorbed polymer layer thickness on the effective solids loading should be considered. This factor becomes especially important when the adsorbed polymer layer thickness is comparable to the particle size. Based on the Krieger-Dougherty equation [22]:

$$\phi_{\text{eff}} = \phi\left(1 + \frac{L}{2a}\right)^3 \tag{14}$$

ϕ_{eff} is the effective solids loading, ϕ is the particle solids loading. For the PAA used, the M_w is 1800 and the adsorbed polymer layer thickness is ~2.5 nm. For the PMAA used, the M_w is 15,000 and the adsorbed polymer layer thickness is ~7.3 nm. For the 40 vol% solids loading suspension, the effective solids loading increases to 52% at 2.5 nm polymer adsorption layer thickness. If the polymer adsorption layer thickness is 7.3 nm, the effective solids loading would be 81%, which is impossible to achieve for the Al_2O_3 nanoparticle systems. Clearly, the polymer layer adsorption can cause drastic effective solids loading increase and pose challenges in creating a high solids loading suspension for bulk component forming. The impact of the polymer adsorption layer thickness and the choice of the dispersant for a specific suspension has actually been clearly observed in the studied Al_2O_3 nanoparticle system. Based on the rheology measurement, the predicted maximum solid loading is 50.7 vol% for PAA and only 41.5 vol% for PMAA [12]. This explains why we have not been able to achieve >40 vol% solids loading experimentally when the PMAA dispersant is used.

The relative contribution to the repulsive interaction from the electrostatic interaction and the steric interaction can be obtained by comparing Figs. 2 and 4. At the greatest electric double layer thickness of 0.66 nm, the repulsive interaction energy from the electrostatic interaction is ~14kT. As the particle–particle separation distance increases, this repulsive energy quickly decreases to almost zero at 3.0 nm particle–particle separation distance. For the steric interaction, the repulsive energy can be as high as 140kT and is effective up to 6.0 nm particle–particle separation distance. So, the steric stabilization is a much more effective approach in stabilizing the Al_2O_3 nanoparticle system. One caution is that the steric stabilization is not always independent. Because of the surface charge of most nanoparticles in water (Al_2O_3 serves as an example), the polymer chains must have appropriate functional group (such as –COOH group of PAA and PMAA) to dissociate into a polar polymer for adsorption onto the nanoparticles (–COO$^-$ group of PAA and PMAA). Subsequently, polyelectrolyte polymers are often used in most nanoparticle suspensions. The electrostatic stabilization and steric stabilization will likely co-exist as electrosteric stabilization.

2.4. Depletion interaction energy

According to the pragmatic theory, the depletion interaction energy $E_{\text{dep}}(h)$ between two soft spheres of radius a at a separation h is given by [24]:

$$E_{\text{dep}}(h) = 2\pi a \frac{\mu_1 - \mu_1^0}{\nu}\left(\Delta - \frac{h}{2} + L - q + p\right)^2 \tag{15}$$

when $\Delta \ll a$, $h \ll a$ and where Δ is the depletion layer thickness, p is the degree of interpenetration between the free and adsorbed polymer chains, q is the compression of the grafted polymer layer, μ_1 is the chemical potential of the dispersing medium at a volume fraction of free polymer ϕ_p, and μ_1^0 is the corresponding value at $\phi_p = 0.0$. $\mu_1 - \mu_1^0$ can be calculated from the Flory-Huggins equation [24]:

$$\frac{\mu_1 - \mu_1^0}{kT} = \ln(1 - \phi_p) + \phi_p\left(1 - \frac{1}{r}\right) + \chi\phi_p^2 \tag{16}$$

where r is the number of statistical segments per chain and can be calculated according to:

$$r = \left(\frac{0.408s}{CM_s}\right)^2 M_w \tag{17}$$

s is the projected length of each repeating unit, C is a constant based on the unperturbed radius of gyration in water and the polymer molecular weight M_w [25,26], M_s is the molecular weight of the repeating unit.

For the Al_2O_3 nanoparticle system with PAA and PMAA, p and q are generally small and is assumed to cancel out with each other, Δ can be assumed approximately as 1.0 nm, s is approximately 2.5 Å, and ϕ_p is approximately 0.0134 based on the potentiometric titration. The depletion interaction energy $E_{\text{dep}}(h)$ can be calculated based on L and M_w and the results are shown in Fig. 5. Interestingly, the depletion attractive energy is very dispersant dependent. For short chain polymers, the effective interaction energy distance is short but the magnitude

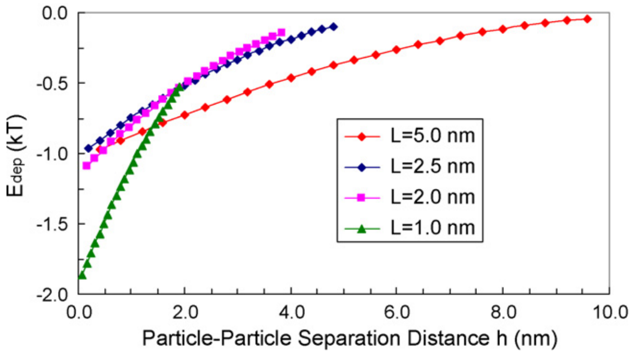

Fig. 5. The depletion interaction energy change vs. particle–particle separation distance h in the studied Al_2O_3 nanoparticle systems.

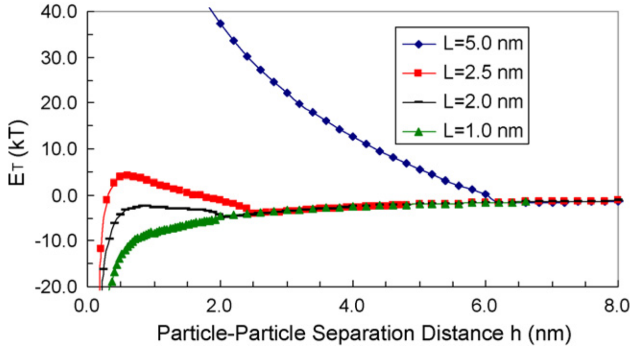

Fig. 6. The depletion interaction energy change vs. particle–particle separation distance *h* in the studied Al_2O_3 nanoparticle systems.

of the attractive energy is higher. As the polymer chain length and thus the polymer adsorption layer thickness increase, the depletion interaction energy first decreases and then increases in the absolute value. The transition happens between 2.0 and 2.5 nm polymer layer thicknesses. This means there is an optimal balance between the polymer adsorption layer thickness and the depletion energy. This balance can be best explained by the free polymer volume fraction. For the short polymer dispersant chain (small *L*), there will be more free polymers because of fewer adsorption points along the polymer backbone. In the meantime, there is also less polymer–polymer induced attraction when the polymer chains are depleted from the space in-between the particles. As a result of these different effects, there is a depletion energy minimum when polymer chain length is considered.

From Figs. 1 and 5, it clearly shows that the van der Waals attraction energy is much higher than the depletion energy (several *kT* versus 1–2*kT*). The van der Waals attraction is the dominating factor in destabilizing the system and should be the focus in dispersing the Al_2O_3 nanoparticle systems.

2.5. Total interaction energy

To evaluate the stability of a nanoparticle suspension, all the above interaction energies need to be considered. With the understanding that the additive rule may not always be applicable to the system, the quantification of the total interaction energy by summing all the interaction energies can serve as a good guide for nanoparticle suspension stability prediction. Based on this consideration, the total interaction energy as a function of Al_2O_3 particle–particle separation distance *h* has been calculated as shown in Fig. 6. Because the effect of the electric double layer is comparatively small, $1/\kappa$ is assumed to be 0.5 nm. As it shows, the total interaction energy is a strong function of the polymer adsorption layer thickness. As the polymer adsorption thickness increases from 1.0 to 5.0 nm, the total interaction energy changes from attraction to repulsion. Most strikingly, the magnitude of the total interaction energy is much higher for the suspension with 5.0 nm polymer adsorption layer thickness. Since $E_T(h)$ should be several times of *kT* to resist coagulation when the particle–particle separation distance *h* is small, the Al_2O_3 nanoparticle suspension will not be stable unless the polymer adsorption layer thickness is 2.5 nm or higher. Using Eq. (13), M_w should be $\geq$1736. This value is extremely close to our experimentally identified optimal value of M_w 1800 [12,13]. As to the nanoparticle suspension flocculation, it will not be an issue for the studied system when *L* is greater than 2.5 nm since the depth of the secondary minimum is less than 2*kT*. With the steric stabilization, the secondary minimum may completely disappear at high *L*; flocculation is unlikely to occur.

Nanoparticles need to be effectively stabilized for a dispersed suspension. However, nanoparticles with excessive polymer adsorption pose challenges in achieving high solids loading suspension. From this analysis, it is clear that the fundamental barrier still lies in maintaining the stability of the system and thus preventing coagulation. Sole reliance on creating electrostatic repulsion may not be sufficient. The steric repulsion shows to be a much more effective technique in increasing particle–particle repulsion. Even though high M_w polymer dispersant is beneficial for creating stable Al_2O_3 nanoparticle suspensions, too thick a polymer adsorption layer is not desirable. One consequence is the increase of the effective solids loading and thus the decrease of the particle solids loading. If an appropriate dispersant can be chosen, high solids loading can be obtained for nanoparticles with narrow size distribution. For the Al_2O_3 nanoparticle suspension stabilized with 1800 M_w PAA, 45.0 vol% solids loading has been achieved and the above predictions have been observed [13]. The caution is that the polymer adsorption onto the particle surface should be effectively achieved by choosing proper electrolyte and polymer dispersant. Otherwise, excessive free polymer in the suspension can not only cause depletion flocculation, but more significantly act as an effective barrier for suspension flow during forming.

3. Conclusions

Based on an Al_2O_3 nanoparticle system, different particle–particle interaction energies in the suspension have been quantitatively analyzed. The study found that the dominant attraction is the van der Waals energy in comparison to the depletion attraction of the free polymers. To counteract the attractive energy, the electrostatic stabilization and/or the steric stabilization can be used. With the proper selection of the polymer dispersant chain length, the steric stabilization is a much more effective approach in stabilizing the Al_2O_3 nanoparticle system. Under all the dispersion conditions considered, the particle–particle distance is not the limiting factor in achieving high solids loading if all the particles are well separated. The system is most likely to become unstable when individual particles happen to approach each other too closely. Based on this, it can be concluded that high solids loading nanoparticle suspensions are achievable with good control of different interaction energies.

Acknowledgements

This work is supported by Oak Ridge Associated Universities. Special thanks go to Xiaojing Zhu for helping out on the interaction energy calculation.

References

[1] D.H. Everett, Basic Principles of Colloid Science, Royal Society of Chemistry, UK, 1992.

[2] J.A. Lewis, Colloidal processing of ceramics, J. Am. Ceram. Soc. 83 (10) (2000) 2341–2359.

[3] J. Cesarano Jr., I.A. Aksay, A. Bleier, Stability of aqueous alpha-Al_2O_3 suspensions with poly(methacrylic acid) poly-electrolyte, J. Am. Ceram. Soc. 71 (4) (1988) 250–255.

[4] J.M. Cho, F. Dogan, Colloidal processing of lead lanthanum zirconate titanate ceramics, J. Mater. Sci. 36 (10) (2001) 2397–2403.

[5] D. Napper, Polymeric Stabilization of Colloidal Dispersions, Academic Press, UK, 1983.

[6] W.M. Sigmund, N.S. Bell, L. Bergstrom, Novel powder-processing methods for advanced ceramics, J. Am. Ceram. Soc. 83 (7) (2000) 1557–1574.

[7] A.L. Ogden, J.A. Lewis, Effect of nonadsorbed polymer on the stability of weakly flocculated suspensions, Langmuir 12 (14) (1996) 3413–3424.

[8] Q. Li, J.A. Lewis, Nanoparticle inks for directed assembly of three-dimensional periodic structures, Adv. Mater. 15 (19) (2003) 1639–1643.

[9] J. Cesarano, I.A. Aksay, Processing of highly concentrated aqueous alpha-alumina suspensions stabilized with poly-electrolytes, J. Am. Ceram. Soc. 71 (12) (1988) 1062–1067.

[10] R. Arnold, J.T.G. Overbeek, The dissociation and specific viscosity of polymethacrylic acid, Recueil 69 (1950) 192–206.

[11] Y.Q. Liu, L.A. Gao, Dispersion of aqueous alumina suspensions using copolymers with synergistic functional groups, Mater. Chem. Phys. 82 (2) (2003) 362–369.

[12] K. Lu, C.S. Kessler, Colloidal dispersion and rheology study of nanoparticles, J. Mater. Sci. 41 (17) (2006) 5613–5618.

[13] K. Lu, C.S. Kessler, R.M. Davis, Optimization of a nanoparticle suspension for freeze casting, J. Am. Ceram. Soc. 89 (8) (2006) 2459–2465.

[14] G. Fritz, V. Schadler, N. Willenbacher, N.J. Wagner, Electrosteric stabilization of colloidal dispersions, Langmuir 18 (16) (2002) 6381–6390.

[15] R.J. Hunter, Foundations of Colloid Science, Clarendon Press, UK, 1987.

[16] J. Gregory, Approximate expressions for retarded van der Waals interaction, J. Colloid Interface Sci. 83 (1) (1981) 138–145.

[17] M.N. Rahaman, Ceramic Processing and Sintering, Marcel Dekker, Inc., NY, 2003.

[18] D.J. Shaw, Introduction to Surface and Colloid Chemistry, Butterworth Heinemann, MA, 1991.

[19] D.R. Lide, Handbook of Chemistry and Physics, CRC Press, FL, 1991–92.

[20] G.S. Manning, Limiting laws and counterion condensation in polyelectrolyte solutions. III. An analysis based on the Mayer ionic solution theory, J. Chem. Phys. 51 (8) (1969) 3249–3252.

[21] B. Vincent, P.F. Luckham, F.A. Waite, Effect of free polymer on the stability of sterically stabilized dispersions, J. Colloid Interface Sci. 73 (2) (1980) 508–521.

[22] B. Vincent, J. Edwards, S. Emmett, A. Jones, Depletion flocculation in dispersions of sterically-stabilized particles (soft spheres), Colloids Surf. 18 (2–4) (1986) 261–281.

[23] G.H. Kirby, D.J. Harris, Q. Li, J.A. Lewis, Poly(acrylic acid)-poly(ethylene oxide) comb polymer effects on $BaTiO_3$ nanoparticle suspension stability, J. Am. Ceram. Soc. 87 (2) (2004) 181–186.

[24] A. Jones, B. Vincent, Depletion flocculation in dispersions of sterically-stabilized particles. 2. Modifications to theory and further-studies, Colloids Surf. 42 (1–2) (1989) 113–138.

[25] Y.K. Leong, Depletion interaction in colloidal suspensions: a comparison between theory and experiment, Colloids Surf. 118 (1–2) (1996) 107–114.

[26] J. Philip, O. Mondain-Monval, F.L. Calderon, J. Bibette, Colloidal force measurements in the presence of a polyelectrolyte, J. Phys. 30 (20) (1997) 2798–2803.